THE JOURNAL OF COMPARATIVE NEUROLOGY 379:271–282 (1997)

Activity-Dependent Regulation of Cytochrome b Gene Expression in Monkey Visual Cortex

B. KAMINSKA,[1] **L. KACZMAREK,**[1,2] **S. LAROCQUE,**[1] **AND A. CHAUDHURI**[1]*
[1]Department of Psychology, McGill University, Montreal, Quebec, H3A 1B1 Canada
[2]Nencki Institute, Warsaw, 02-093 Poland

ABSTRACT

The recent demonstration that certain mitochondrial subunits of cytochrome oxidase (CO) are regulated by neuronal activity has stimulated interest in the molecular processes that coordinate nuclear and mitochondrial gene expression following synaptic stimulation. We have studied the constitutive expression and activity-guided regulation of cytochrome b (cyt b), a gene that is encoded by mitochondrial DNA and that was cloned by subtractive hybridization from the lateral geniculate nucleus in the monkey. We have found cyt b mRNA expression in monkey striate cortex to be similar to that of CO activity with regard to the laminar profile and the presence of blobs in the supragranular layers. Layers 2/3, 4C, and 6 contained large numbers of stained cells, many of which were judged to be excitatory neurons, because they showed a Zif268-immunopositive nucleus. We have also found that removal of functional activity reduced cyt b mRNA content in area V1. Columns of reduced cyt b staining were visible after 3 days and were especially striking after 6 days of monocular deprivation. After 3 months of deprivation, the columns lost their contrast and became blurred. Our principal finding, that neuronal activity regulates cyt b levels, suggests that expression of a mitochondrial gene can be affected in a manner similar to that of several known nuclear genes. The differences in cyt b mRNA levels and CO activity after long-term deprivation suggests that some form of differential control is exerted on cyt b. Cyt b expression, therefore, may be used as a marker of altered mitochondrial transcription that is guided by the metabolic demands of active neurons. J. Comp. Neurol. 379:271–282, 1997.

Indexing terms: lateral geniculate nucleus; Zif268; cytochrome oxidase; mitochondrion; plasticity

One of the most widely studied markers of brain metabolic activity is the mitochondrial enzyme cytochrome c oxidase (CO). An elegant demonstration of CO regulation by functional activity is the staining of ocular dominance (OD) columns in monkey striate cortex (Wong-Riley, 1989). Monocular deprivation (MD) has been shown to down-regulate CO levels in OD columns that represent the deprived eye (Horton and Hubel, 1981; Horton, 1984; Wong-Riley and Carroll, 1984; Hevner and Wong-Riley, 1990; Rosa et al., 1991). An additional feature of CO staining is its uneven distribution in the superficial layers of the visual cortex in Old World monkeys (Horton, 1984). These so-called "puffs" or "blobs" of intense CO levels are believed to demarcate cortical regions that normally exhibit enhanced metabolic activity (Wong-Riley et al., 1989; Hevner et al., 1992).

The correlation of CO levels with functional activity in neurons is intriguing because of the structural complexity of the CO holoenzyme and the coding of its various subunits by two spatially separated genomes. It is known that 10 of the 13 subunits in mammalian CO are encoded by nuclear genes, whereas the remaining 3 subunits are encoded by mitochondrial (mt) DNA (Kadenbach et al., 1987). Hevner and Wong-Riley (1991, 1993) have shown that both nuclear and mt CO genes are down-regulated by removal of afferent input. Although the effect on the nuclear subunits is likely to be mediated by an intracellular cascade of second messengers and transcription factors

Contract grant sponsor: Medical Research Council of Canada; Contract grant number: MRC-MA12685; Contract grant sponsor: Natural Sciences and Engineering Research Council of Canada; Contract grant number: NSERC-OGP0155482.

*Correspondence to: Avi Chaudhuri, Department of Psychology, McGill University, 1205 Dr. Penfield Avenue, Montreal, QC, H3A 1B1 Canada. E-mail: avi@hebb.psych.mcgill.ca

Received 10 January 1996; Revised 10 October 1996; Accepted 10 October 1996

(Morgan and Curran, 1991; Struhl, 1991), the molecular mechanisms that guide transcriptional control of the mitochondrial compartment are less clear. Although it has been suggested that the two genomes that encode CO are regulated in concert (Wiesner et al., 1994), there is also evidence for a disengagement of the two regulatory mechanisms (Van Itallie et al., 1993; Hevner and Wong-Riley, 1993).

To further our knowledge of bigenomic enzyme regulation, it would be useful to examine the linkage of other mitochondrial components to neural activity. Cytochrome b (cyt b)—a mitochondrial protein that is also involved in bioenergetic metabolism as part of the respiratory chain—is a suitable candidate for this purpose. It is encoded entirely by mitochondrial DNA—a 16.5 kb circular entity that encodes subunits of a few other respiratory chain proteins as well as 2 rRNAs and 22 tRNAs (Tzagaloff and Macino, 1979; Clayton, 1984; Gadaleta et al., 1989; Van Itallie et al., 1993). Cyt b is transcribed as polycistronic RNAs from the entire mitochondrial DNA, cut into precursor molecules, and cleaved further into individual mRNAs that encode the proteins. The 3.6 kb cyt b precursor RNA contains not only the cyt b mRNA but also that of NADPH-ubiquinone oxidoreductase subunit 5 (Van Itallie et al., 1993). Cyt b combines with nuclear-encoded cytochrome c1 to participate in the formation of complex III of the electron transport chain.

We report here on the constitutive expression of cyt b mRNA in monkey visual cortex and its transcriptional regulation by functional activity. Although we have found similarities between cyt b mRNA expression and CO activity, there were some noteworthy differences as well. Our principal finding that neuronal activity regulates cyt b levels shows that expression of a gene that is encoded by the mitochondrial compartment can be affected in a manner similar to that of several known nuclear genes. Cyt b expression, therefore, may be used as a marker of activity-guided regulation of the mitochondrial genome in neurons.

MATERIALS AND METHODS

Animal preparation

We used adult male vervet monkeys (*Cercopithicus aethiops*) that were obtained from a feral colony in St. Kitts (West Indies) for this study. Animals were treated with different conditions of light exposure as follows: normal light adapted (n = 4); MD for 1 day (n = 2), 3 days (n = 1), 6 days (n = 2), and 3 months (n = 2). The short-term MDs (1 and 3 days) were produced by intravitreal tetrodotoxin (TTX; 1 mg/ml, 30 µl) injection, whereas enucleation was used to produce longer periods of monocular deprivation. For all surgical procedures, the animal was first sedated with ketamine (10 mg/kg, i.m.) followed by sodium pentobarbital (2 mg/kg, i.v.). Brain tissue from these animals was used for several additional studies along with the present one.

At the conclusion of the exposure period, all animals were sedated with ketamine, removed from their cages, and killed with an overdose of sodium pentobarbital. The chest was then opened with a bilateral incision along the rib cage, and the heart was exposed. A small incision was made on the dorsal tip of the right atrium, and blood was drained for a few seconds to relieve pressure. The animals were then perfused with diethyl pyrocarbonate (DEPC)-treated 0.1 M phosphate-buffered saline (PBS) through the left ventricle until completely exsanguinated. The descending aorta was clamped shortly after onset of perfusion. The brain was removed and blocked along the midline followed by a coronal block of both hemispheres at the lunate sulcus and at the central sulcus. In two normal animals, tissue from various cortical segments—V1, V4, IT, MT, 7, and FEF—was dissected and preserved separately for RNA extraction and Northern analysis. In all cases, the tissue was rapidly frozen by immersion in 2-methylbutane that was maintained at −50°C in a dry-ice bath.

Tissue preparation

To prepare cDNA libraries, coronal sections of lateral geniculate nucleus (LGN) tissue were made in a cryostat at a thickness of 50 µm. While the sections were frozen, the magnocellular (M) and parvocellular (P) compartments were dissected under a stereomicroscope and collected in separate microfuge tubes. A total of six LGN from three animals were processed in this manner to yield approximately 100 mg of tissue in each vial. For Northern analysis of total LGN, the same general procedure was applied on two LGN but without further dissection of the magno- and parvocellular compartments.

For in situ hybridization histochemistry (ISHH), tissue blocks were also sectioned in the coronal plane, but at a thickness of 15 µm, thaw mounted on polylysine subbed slides, and air dried overnight. The slides were prepared by first baking overnight at 200°C and by then dipping in poly-L-lysine solution (Sigma, St. Louis, MO; catalog no. P 8920), according to the manufacturer's procedure. The cortical region that was of particular interest to us in this study was area V1 from normal animals and those treated with monocular exposure for variable periods, as above. All blocks and sections were maintained at −80°C until further processing.

cDNA cloning

The procedures for cDNA library construction and subtractive hybridization that we employed on monkey LGN compartments have been reported previously (Chaudhuri et al., 1993). Briefly, 2.5 µg of mRNA were extracted and purified from each of the M- and P-LGN tissue samples by using oligo-dT cellulose separation (Stratagene, La Jolla, CA). cDNA libraries were then prepared in the λ_{ZAP} cloning vector by using techniques described in the manufacturer's protocol (Stratagene). Each original M- and P-cDNA library contained $>1 \times 10^6$ pfu/ml prior to amplification. Single-stranded DNAs were obtained from both M- and P-LGN cDNA libraries upon which subtractive hybridization was performed in order to remove sequences that were common to both cDNA pools (Hedrick et al., 1984; Prasad and Cynader, 1994). DNA from the control tissue (P-LGN) was photobiotinylated, and removal of hybridized sequences was accomplished by streptavidin binding and phenol-chloroform extraction. The remaining unique single-stranded cDNA fraction (M enriched) was converted to a double-stranded form and transformed in DH5α bacterial cells.

To analyze the subtracted library, we first performed a restriction digest to identify those clones containing large inserts (>600 bp). From this sample, we selected a clone (M54) based on initial results of high levels of expression obtained with in situ hybridization analysis of monkey LGN sections (Kaczmarek et al., 1995). We were also interested in identifying those clones that showed expres-

sion in visual cortex, as revealed by Northern and in situ hybridization analysis. Clone M54 satisfied these criteria; therefore, it was chosen for further study.

Sequence analysis and characterization

DNA sequencing of M54 was performed with an automatic sequencer (373A; Applied Biosystems) using universal primers specific to the pBluescript-SK$^+$ vector and with a custom-made primer (5′-ATTGTGGATGCTAGTTGACC-3′) specific to an internal sequence. The sequencing was repeated twice with both universal and internal primers. The Blast sequence analysis program was used to search for sequence homologies at the National Center for Biotechnology Information (NCBI) databank using the Blast network service (Altschul et al., 1990).

For Northern analysis, RNAs were extracted (Chomczynski and Sacchi, 1987) from LGN as well as various cortical areas (V1, V4, IT, MT, 7, and FEF). The RNA was then electrophoresed through 1% denaturing agarose gel and transferred onto a nylon membrane (Hybond N$^+$; Amersham, Chicago, IL), as previously described (Kaminska et al., 1994). Specific mRNA was detected by hybridization with M54 cDNA probe labeled by a random primer method using α^{32}P dCTP (Redi-prime; Amersham). The membranes were then exposed to x-ray films (MP; Amersham) with intensifying screens.

ISHH

Plasmid DNA was isolated with Wizard minipreps (Promega) and linearized by digestion with BamHI or XhoI. The corresponding antisense and sense RNA probes were obtained by using T7 or T3 RNA polymerases, respectively. We used both radiolabeled and digoxigenin (dig)-conjugated probes to visualize the distribution of M54 mRNA in visual cortex and LGN. The radiolabeled probes were obtained with ^{33}P-UTP (NEN-Dupont, Boston, MA), whereas the dig-conjugated probes were prepared by incorporation of dig-11-UTP (Boehringer Mannheim, Indianapolis, IN).

Glass-mounted sections were thawed at room temperature for 10 minutes and postfixed in 4% paraformaldehyde (PFA) for 10 minutes. The PFA solution, like all others used in this protocol, was made with Milli-Q-purified (Millipore, Bedford, MA) water treated with DEPC overnight and autoclaved. The sections were washed three times in 2 × standard saline citrate (SSC; 1 × SSC = 0.15 M sodium chloride and 0.015 M sodium citrate, pH 7.0) and incubated in hybridization solution (50% deionized formamide, 0.6 M sodium chloride, 10 mM Tris-HCl, pH 7.5, 1 × Denhardt's solution, 1 mM EDTA, pH 8.0, 0.1 mg/ml salmon sperm DNA, 0.1 mg/ml tRNA, 0.1 g/ml dextran sulfate) containing either 10^7 cpm/ml radiolabeled or 100 ng/ml dig-labeled probe. We applied 70 µl of this solution to each slide, coverslipped the section, and incubated overnight at 42°C in a humid chamber containing 50% formamide in 2 × SSC. After incubation, the sections were washed three times in 2 × SSC for 5 minutes followed by incubation in a solution containing 10 µg/ml of RNAse A, 0.5 M sodium chloride, 10 mM Tris-HCl, pH 7.5, and 1 mM EDTA for 30 minutes at 37°C. After a single wash in 1 × SSC for 5 minutes, the sections were incubated at 55°C in a solution containing 0.1 × SSC for 30 minutes.

For radiolabeled probes, the slides were dipped in deionized water, dehydrated in graded ethanols (70%, 95%, 100%) containing 0.3 M ammonium acetate, air dried, and exposed to Hyperfilm β-max (Amersham) for 4 days at room temperature. For dig-labeled probes, the slides were equilibrated in 0.1 M Tris-HCl and 0.15 M NaCl, pH 7.5 (buffer 1), for 1 minute followed by a 30 minute incubation in buffer 1 + 2% normal goat serum at room temperature. The hybridized complex was visualized by an immunocytochemical (ICC) procedure. Slides were placed in newly prepared solution from the previous step with the addition of 1/500 alkaline phosphatase-conjugated anti-dig antibody (catalog no. 1 093 274; Boehringer Mannheim) for 2 hours followed by a single wash for 5 minutes in buffer 1 and two washes in 0.1 M Tris-HCl, 0.1 M NaCl, and 0.05 M $MgCl_2$, pH 9.5 (buffer 2). The final step involved colorimetric development with either NBT/X-phosphate in buffer 2 or fast red in 0.1 M Tris-HCl, pH 8.2, according to the manufacturer's protocol (Boehringer Mannheim). The sections were coverslipped with Aquamount (VWR).

Cyt b ISHH/Zif268 ICC double staining

Coronal sections were first treated with nonradioactive ISHH by using dig-conjugated cyt b RNA probe, as above. The colorimetric development in this case involved fast red to provide a red reaction product. After the ISHH steps were completed and an adequate signal was observed, the same tissue sections were then treated with immunostaining for Zif268. The sections were first equilibrated in PBS for 5 minutes and incubated overnight in primary antibody solution (polyclonal anti-Zif268; a gift from R. Bravo, Bristol-Myers Squibb, Princeton, NJ). Our ICC protocol has been described previously in detail (Chaudhuri et al., 1995). It is important to avoid adding Triton X-100 to the primary antibody solution and subsequent washes until the secondary antibody step. The reaction complex was visualized by diaminobenzidene (DAB) substrate.

CO histochemistry

CO histochemistry was performed according to a protocol described by Dyck and Cynader (1993). Briefly, sections were fixed for 5 minutes in 4% paraformaldehyde in 0.05 M phosphate buffer, pH 7.2, followed by two rinses in buffer for 2 minutes each. The slides were then placed in 0.05 M phosphate buffer containing 0.01 g/ml sucrose, 0.5 mg/ml nickel-ammonium sulphate, 0.25 mg/ml DAB, 0.15 mg/ml cytochrome c, 0.1 mg/ml catalase, and 2.5 mM imidazole (all reagents from Sigma). The reaction was stopped by immersion in phosphate buffer, after which the sections were dehydrated and coverslipped. Adjacent sections were also stained for Nissl substance with 1% cresyl violet.

Image analysis and documentation

Film autoradiograms were photographed by using a Leica MZ6 stereomicroscope and camera attachment with Tmax film. High-magnification photomicrographs were taken with a Leica DMLB compound microscope using Ektachrome 100 film. To compare stained features in adjacent sections, digitized images were captured with a Sony monochrome CCD camera. The images were then analyzed on a Macintosh 8100/100 computer using the public domain NIH Image program and Adobe Photoshop. We used both external boundaries and internal fiducial markers for aligning consecutive sections that were treated with different staining procedures. Where necessary, images were digitally superimposed to establish the spatial relationships among stained features.

```
CGGCACGAGA ATGAATCTGA GGTGGGTACT CCATTGGCAA CCCCACCCTT  50
TCACGATTCT TCACCCTACA CTTTATTCTA CCTTTCATTA TCACCGCTCT 100
TACAATAGTC CATCTGCTAT TCCTACACGA AACAGGATCA AACAACCCCT 150
GCGGAATCTC ATCAGACTCA GACAAAATCC CCTTCCACCC CTACTACACA 200
ATTAAGGATA TCCTAGGCCT AGTCCTCCTC CTCTTCATCC TAACAACACT 250
AACACTACTC TCACCCAACC TCCTAAACGA CCCAGACAAC TACATCCCAG 300
GCGACCCACT AAATACCCCT CCACACATCA AACCAGAGTG ATACTTCCTA 350
TTTGGATACG CAATTCTACG ATCTGTTCCT AATAAACTAG GGGGCGTACT 400
AGCACTCTTC CTTTCAATCC TCATCCTATC TATTATCCCC ACACTTCATA 450
ATTCCAAACA ACAAAGCATA ATATTCCGCC CACTTAGCCA ATTCCTGTTC 500
TGATTCCTAA TTACAACCCT ATTAACCCTC ACCTGGATCG GAAGTCAGCC 550
AGTAAGCCAA CCCTTCATTT TTATTGGTCA ACTAGCATCC ACAATATACT 600
TCACCACAGT TCTAATCCTG ATACCACTAA CCTCCCTAAT CGAAAATAAC 650
CTACTCAGAT GGACTTGAAG AAAAAAAAAA AAAAA
```

Fig. 1. Nucleotide sequence of cytochrome b (cyt b) cDNA. The cloned cDNA fragment, which was 685 bp long, corresponded to the 3′ end of native mRNA, as indicated by the presence of a polyadenylated tail and by nucleotide correspondence to cyt b in several species.

RESULTS

Molecular characterization of monkey cyt b cDNA

The nucleotide sequence of the cloned cDNA fragment is presented in Figure 1 .(NCBI accession no. U63128). Database search performed with the NCBI Blast program revealed that the clone had clear homology to mitochondrial DNA coding for cyt b in a number of mammalian species. It appears that the cDNA fragment, which was 685 bp long, corresponded to the 3′ end of native 1.2 kb mRNA, as indicated by the presence of a polyadenylated tail and by nucleotide correspondence to cyt b in several species. To our knowledge, this gene has not been cloned previously in the monkey. Comparison with various mammalian cyt b sequences deposited in the NCBI database revealed that our clone had the highest homology to primates (gorilla, 79%; orangutan, 77%; chimpanzee, 77%; human, 76%) and was somewhat lower than that of other mammals (<75%)

To identify mRNA species recognized by the cyt b cDNA probe, Northern blot analysis was performed on RNAs isolated from the LGN as well as various areas of vervet monkey visual cortex. The analysis revealed the presence of a major RNA transcript that was approximately 1.2 kb long and an additional one that was about 3.6 kb long and had lower abundance (Fig. 2). The levels of cyt b mRNA did not differ significantly among different cortical structures when normalized for total RNA loading. An ethidium-bromide-stained gel showing RNA loading within lanes is depicted at the bottom in Figure 2.

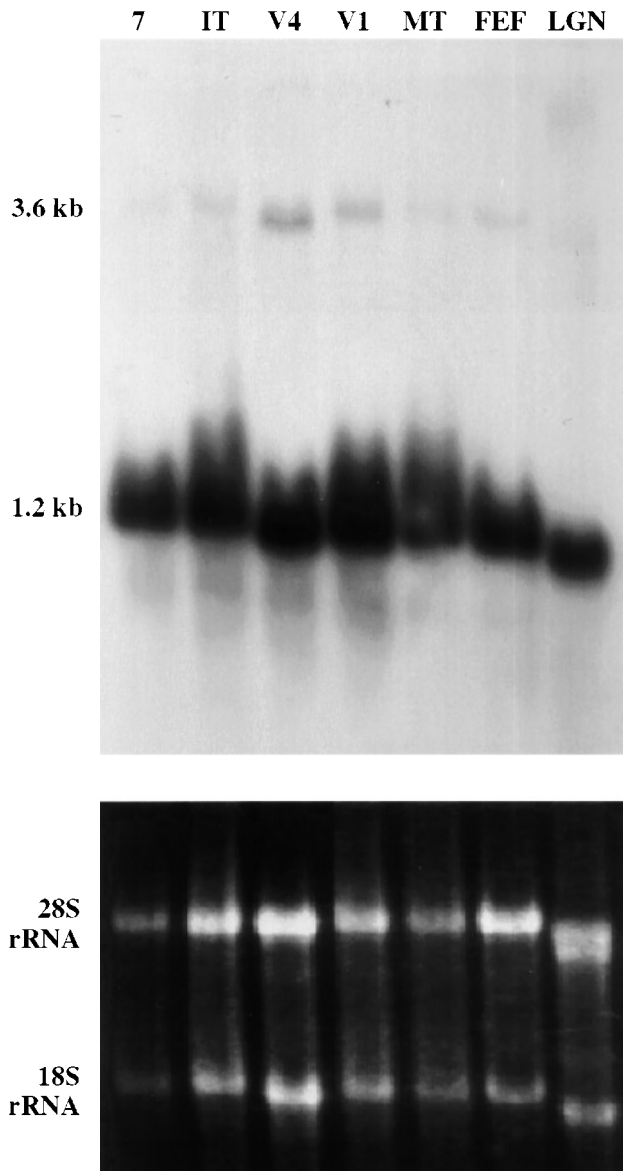

Fig. 2. Northern blot analysis of RNAs isolated from the lateral geniculate nucleus (LGN) and various areas of the vervet monkey visual cortex. The cyt b probe detected the presence of a major RNA transcript that was approximately 1.2 kb long and an additional transcript that was about 3.6 kb long and had lower abundance (**top**). Band intensities did not differ significantly among different cortical structures when normalized to total RNA loading, which was estimated by using ethidium-bromide staining (**bottom**).

Laminar and cellular distribution of cyt b mRNA in area V1

We have examined the distribution of cyt b mRNA in area V1 by means of ISHH with a radiolabeled RNA probe. We employed three kinds of controls to ascertain the specificity of the signal generated by the antisense cyt b probe. These included comparison to hybridization with the sense probe, hybridization with other arbitrary probes chosen from the cDNA library, and hybridization to RNase A-treated sections. All three control procedures showed negligible staining when compared with the antisense probe.

Figure 3 presents a collage of three adjacent coronal sections that were treated with Nissl staining (cresyl violet), cyt b ISHH, and CO histochemistry. Differences in cyt b expression among different layers were discernible—They were highest in layers 2/3, 4C, and 6 and were significantly weaker in layers 1, 4B, and 5. This profile was similar to that seen with CO staining.

The cellular localization of cyt b mRNA was studied by means of nonradioactive ISHH, which involved a dig-conjugated RNA probe. A key issue that we attempted to

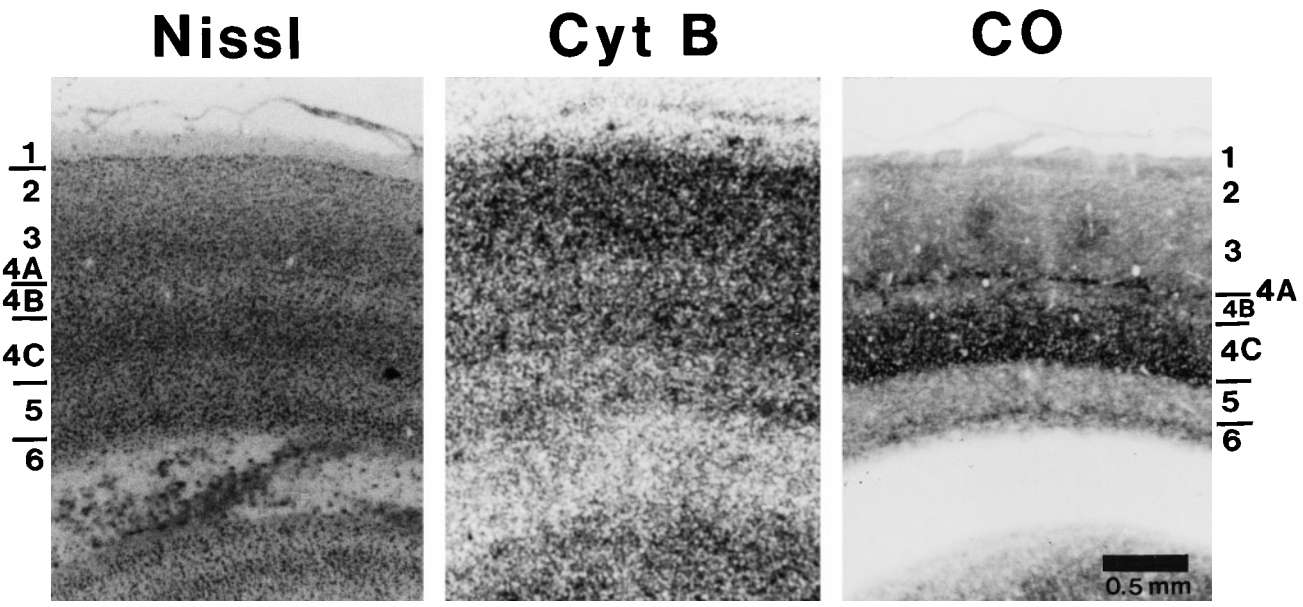

Fig. 3. Comparison of cyt b mRNA expression, cytochrome oxidase (CO) activity, and Nissl staining in area V1. Cyt b mRNA was detected with a radiolabeled RNA probe that was generated from the cloned cDNA fragment and compared to adjacent sections treated with Nissl (cresyl violet) and CO staining. The photomicrographs were spatially aligned by using external boundaries and internal landmarks. Cyt b mRNA expression is elevated in layers 2/3, 4C, and 6 compared with other layers. Comparison with CO staining showed a similar profile of laminar staining.

address by using this method was the subcellular compartment of cyt b staining, i.e., whether the hybridization signal was localized to cell bodies exclusively or also included dendritic processes. Figure 4A shows a collage of four discrete segments along the entire thickness of area V1 that was stained for cyt b mRNA and was revealed by alkaline phosphatase/NBT to produce a dark blue reaction product. It can be seen here that much of the dig-RNA labeling was located in cell bodies, as evidenced by the hollow appearance of cells due to cytoplasmic staining around a negatively stained nucleus. Layers 2/3, 4C, and 6 showed large numbers of stained cells and was therefore consistent with the elevated signals observed with the radiolabeled probe in these layers. The stained cells, however, appeared to be surrounded by weakly stained neuropil (Fig. 4B). We also noted the presence of a few stained cells scattered throughout layer 1. A few neurons with large somata were stained in layers IVB and VI (see, e.g., Fig. 4D, black arrowhead).

To confirm that the cells stained with the dig-conjugated RNA probe were indeed neurons, we employed a double-labeling strategy that combined nonradioactive ISHH for cyt b along with immunostaining for Zif268 on the same section. We chose to stain for Zif268 because it has been shown to be exclusively associated with neurons (Chaudhuri et al., 1995) and because it is largely confined to the nucleus, where it functions as a transcription-regulating protein. This feature of Zif268 localization would allow us to visualize double-labeled neurons easily due to spatial separation with cyt b mRNA staining in the cytoplasm. To visualize the Zif268-immunopositive complex, we used a DAB reaction that produced a light brown product. To contrast with this, the dig-ISHH cyt b product was revealed by fast red substrate for alkaline phosphatase to produce a red complex.

Figure 4C,D shows the results from this double-labeling procedure in layers 2 and 6, respectively. Numerous double-labeled cells (Fig. 4C,D, black arrowheads) are clearly visible, i.e., an immunostained nucleus (Zif268) surrounded by a stained cytoplasmic ring (cyt b). However, a few cells were also present in these sections in which cyt b staining was accompanied by poor nuclear staining (Fig. 4C,D, white arrowheads). Contrary to the NBT substrate, the fast red reaction resulted in a speckled deposition of the hybridization signal in the perinuclear region of the cell body.

Activity-dependent expression of cyt b mRNA

We have examined the dependence of cyt b expression on visual input in area V1 with an MD paradigm. Figure 5 shows the effects of different MD durations on cyt b mRNA distribution in coronal section. The earliest time point at which regional variations in cyt b expression were visible occurred after 3 days of MD and were revealed as a series of blobs and columns. The changes in cyt b expression with deprivation were most prominent after 6 days of MD and became reduced after 3 months. In all cases, the contrast between columns of high and low expression was greatest in layer 4C. We have observed this effect in two animals per time point, except for the 3 days of MD condition, where only one monkey was used.

We wanted to compare the cyt b mRNA profile with that of CO activity to determine whether blobs and columns with both markers were spatially correlated. To facilitate such comparison of the blobs, we overlapped digitized images from adjacent sections. Figure 6A shows two such adjacent tangential sections of flattened striate cortex that were stained for CO activity and cyt b mRNA expression.

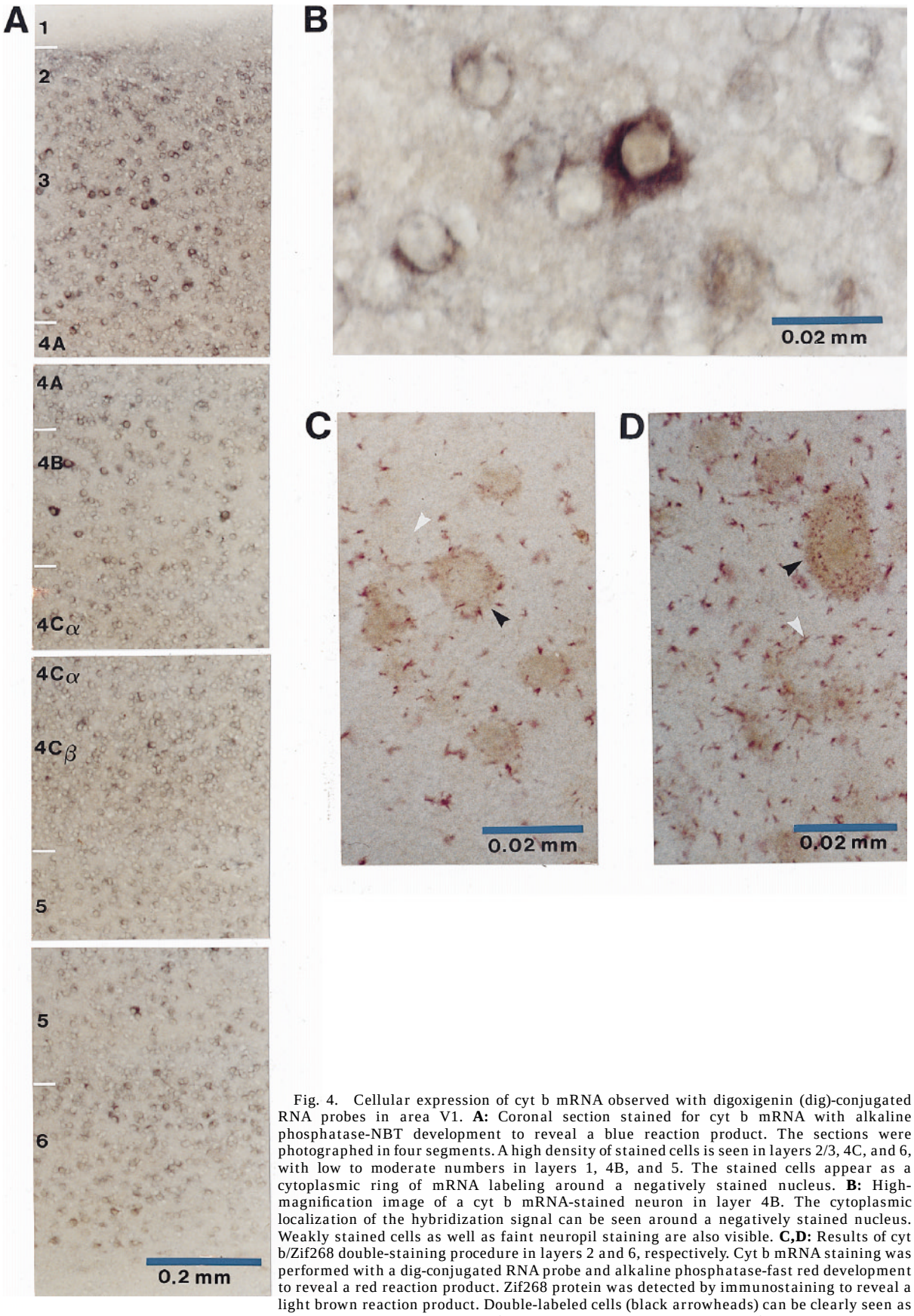

Fig. 4. Cellular expression of cyt b mRNA observed with digoxigenin (dig)-conjugated RNA probes in area V1. **A:** Coronal section stained for cyt b mRNA with alkaline phosphatase-NBT development to reveal a blue reaction product. The sections were photographed in four segments. A high density of stained cells is seen in layers 2/3, 4C, and 6, with low to moderate numbers in layers 1, 4B, and 5. The stained cells appear as a cytoplasmic ring of mRNA labeling around a negatively stained nucleus. **B:** High-magnification image of a cyt b mRNA-stained neuron in layer 4B. The cytoplasmic localization of the hybridization signal can be seen around a negatively stained nucleus. Weakly stained cells as well as faint neuropil staining are also visible. **C,D:** Results of cyt b/Zif268 double-staining procedure in layers 2 and 6, respectively. Cyt b mRNA staining was performed with a dig-conjugated RNA probe and alkaline phosphatase-fast red development to reveal a red reaction product. Zif268 protein was detected by immunostaining to reveal a light brown reaction product. Double-labeled cells (black arrowheads) can be clearly seen as an immunopositive nucleus (Zif268 protein) surrounded by a ring of cytoplasmic staining (cyt b mRNA). Some cyt b^+ cells that were weakly immunopositive were also present (white arrowheads).

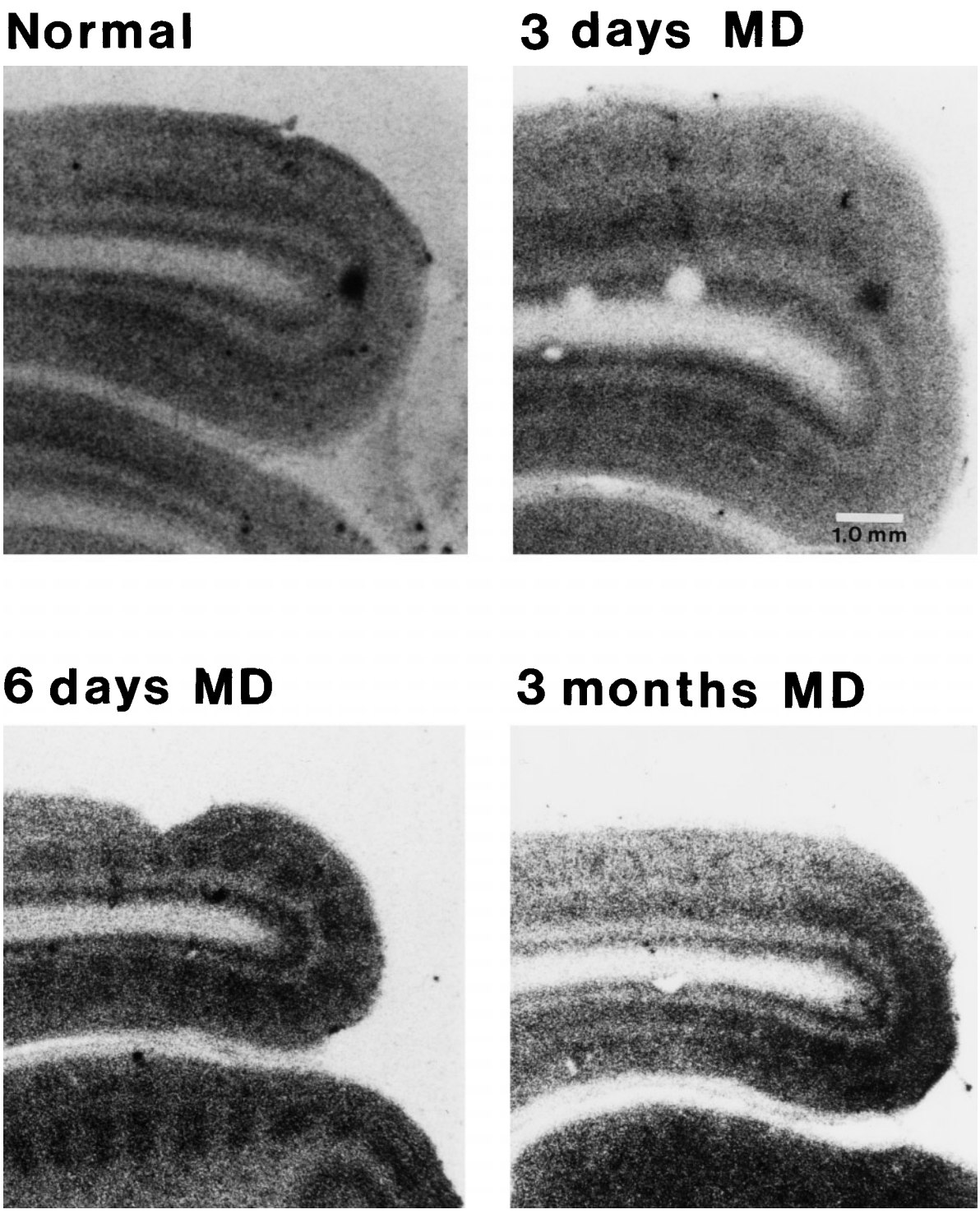

Fig. 5. Effect of monocular deprivation (MD) on cyt b mRNA expression. Representative coronal sections are shown from animals treated for various periods of monocular deprivation. Columns of reduced cyt b mRNA staining were clearly discernible after as little as 3 days of MD. After 6 days of MD, the columns showed greater contrast and became especially striking in layer 4. However, after 3 months of MD, the columns were less distinct and became spatially blurred.

These sections, which were taken from layer 2 of an animal with 6 days of MD, revealed a pattern of blobs with both markers. The spacing between the centers of the blobs averaged 500 μm in both cases. The cyt b- and CO-stained images were then aligned and digitally superimposed with the aid of fiducial points that had been placed in the tissue

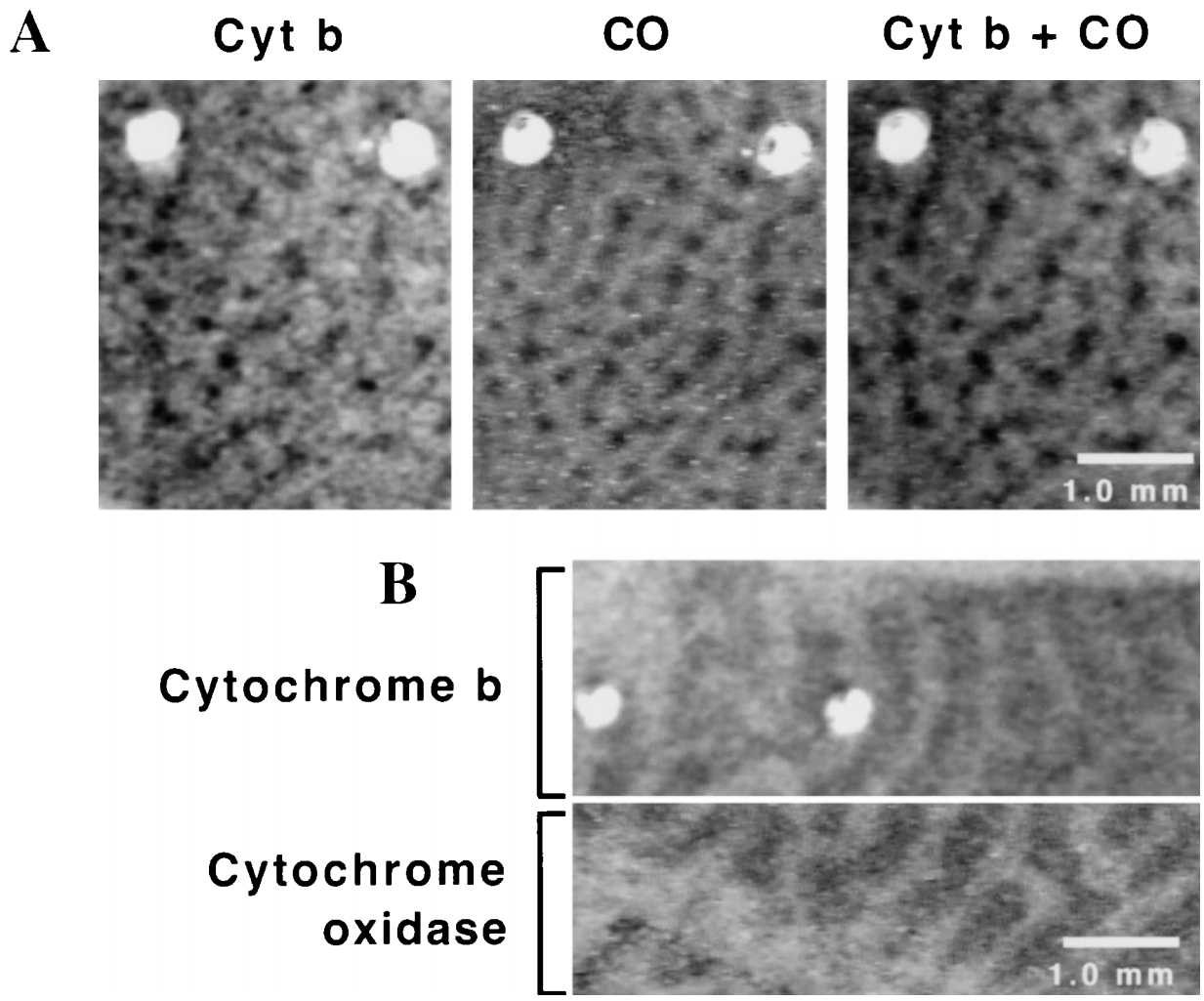

Fig. 6. Comparison of cyt b mRNA and CO staining profiles. Two adjacent tangential sections of flattened striate cortex were stained for CO activity and cyt b mRNA expression to see whether blobs and columns of enhanced cyt b correlated with increased functional and metabolic activity. **A:** Sections taken from layer 2 of an animal at 6 days of MD show a pattern of blobs with both markers. The spacing between the centers of the blobs averaged 500 μm in both cases. The cyt b- and CO-stained images were aligned on the basis of fiducial points and were digitally superimposed, revealing both blob patterns to be spatially coincident (A, right). **B:** Sections taken from layer 4C of the same animal as in A (6 days of MD) were aligned on the basis of fiducial points. The two digitized images were then segmented and juxtaposed, revealing an ocular dominance pattern that was clearly aligned between the two sections. Columns of elevated cyt b mRNA expression (top) showed spatial continuity with those in the CO pattern from an adjacent region (bottom).

block during sectioning. This procedure revealed that blobs stained by CO and cyt b were spatially coincident (Fig. 6A, right). Indeed, we have found precise spatial correspondence throughout opercular V1 between blobs of cyt b expression and CO staining in both of the animals with 6 days of MD.

To compare the columnar patterns, we again employed digitized images to examine the spatial coincidence among columns revealed by the two markers in layer 4C. Two adjacent flattened sections taken from the same animal (6 days of MD) were again aligned on the basis of fiducial points. The two digitized images were then segmented and juxtaposed, revealing an OD pattern that was clearly aligned between the two sections (Fig. 6B), that is, columns of elevated cyt b mRNA expression (shown in Fig. 6B, top) showed spatial continuity with those in the CO pattern from an adjacent region (shown in Fig. 6B, bottom). Together, these results show that CO activity and cyt b mRNA expression in primary visual cortex is spatially coincident with regard to the supragranular blobs as well as the OD pattern in layer 4C.

The linkage of cyt b mRNA expression with functional activity is examined further in Figure 7. Coronal sections of area V1 from animals that received 3 days and 6 days of MD and were treated with cyt b ISHH and CO histochemistry showed similar staining patterns, as discussed above. However, there was a notable difference with long-term deprivation effects. After 3 months of MD, OD columns of high CO activity were very well delineated and showed a striking contrast with neighboring columns. Cyt b mRNA expression, however, was more homogeneous after 3 months of MD in all layers. Indeed, the OD columns in layer 4C were less distinct than in the 6 days of MD

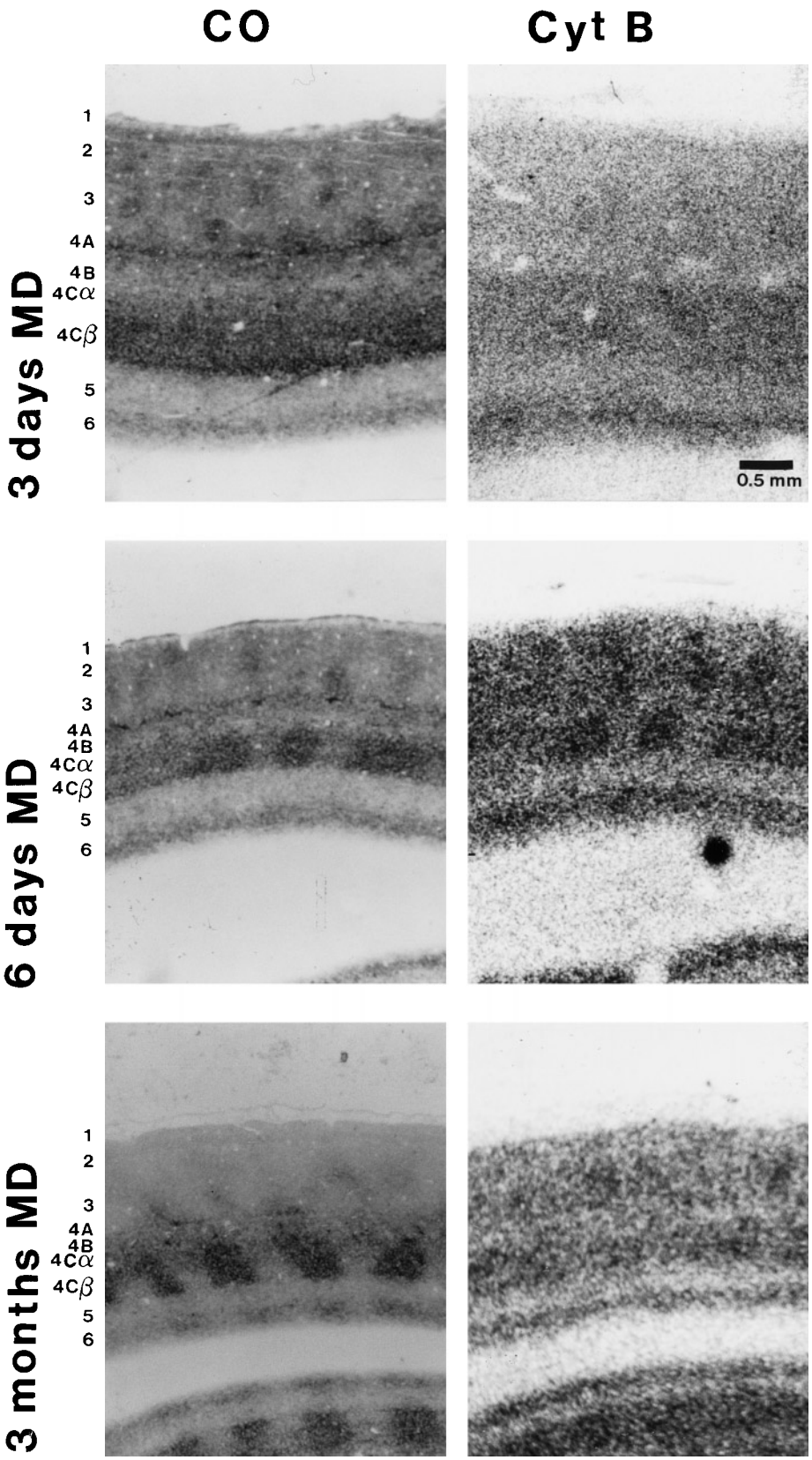

Fig. 7. Laminar and regional analysis of cyt b mRNA expression and CO activity after visual deprivation. Coronal sections from animals treated for 3 days, 6 days, and 3 months of MD and stained for cyt b mRNA and CO activity. After 3 months of MD, ocular dominance columns of high CO activity were very well delineated and showed a striking contrast with neighboring columns, whereas cyt b mRNA expression was more homogeneous.

condition, an effect that we observed throughout the primary visual cortex in two animals for each time point.

DISCUSSION

The transcriptional control of nuclear and mitochondrial genes by functional activity is of interest because of the roles their products play in cellular homeostasis. Cyt b is a key participant in oxidative metabolism, which neurons rely on for their major source of energy, which, in turn, is correlated to functional activity. Primary visual cortex in monkeys is particularly suitable for examining the activity dependent regulation of mitochondrial enzymes because of its high level of neural activity, which can be easily down-regulated by sensory deprivation. Furthermore, the OD architecture of monkey area V1 allows comparison of neighboring cortical areas that differ in activity level.

We have reported here that cyt b, which is encoded entirely by the mitochondrial genome, is down-regulated by removal of functional activity and that its levels in general can be correlated with that of CO activity. We discuss below aspects of cyt b related to its cloning, constitutive expression, and regulation by functional activity. We argue that cyt b mRNA may be useful as a molecular marker of mitochondrial transcriptional events that are guided by the metabolic demands of active neurons.

Analysis and characterization of cyt b

By virtue of high expression levels within the LGN and visual cortex, we have obtained a cDNA clone (M54) whose sequence analysis revealed that it encodes cyt b. We have found that our cloned cDNA fragment represents the 3′ end of cyt b mRNA based on sequence homology with a number of species. In the absence of sequence records from any monkey species in the NCBI database, our characterization of the M54 clone as being cyt b relied on its striking homology to other primate species, including the human cloned sequence (range 76–79%; NCBI database; Bethesda, MD). We performed a similarity search with the same 3′ region of the gorilla cyt b sequence taken from the NCBI database and found that it displayed higher homology with that of other apes (range 86–88%). This suggests an evolutionary transition in nucleotide coding from monkeys to apes.

The 3.6 kb band recognized by the cyt b cDNA probe represented precursor RNA that is also known to contain subunit 5 of NADPH-ubiquinone oxidoreductase (Van Itallie et al., 1993). It has been shown that the processing of this precursor is relatively slow, and the presence of precursor mRNA has been demonstrated in other cells (Van Itallie, 1990; Van Itallie et al., 1993). Nevertheless, levels of the 3.6 kb fragment are significantly lower than cyt b mRNA (1.2 kb) in brain tissue. Indeed, the autoradiogram shown in Figure 2 was overexposed to demonstrate both cyt b and its precursor RNA. This suggests that activity-dependent changes in staining that were observed in area V1 after monocular exposure were largely produced by changes in cyt b mRNA levels rather than the precursor.

Comparison of cyt b mRNA expression and CO activity

We have shown that cyt b mRNA expression in area V1 was spatially coincident with CO activity in both laminar profile and regional inhomogeneities, such as blobs in the supragranular layers. It has been established that CO enzymatic activity is directly related to CO protein levels in brain and muscle tissues (Williams and Harlan, 1987; Hevner and Wong-Riley, 1990). Hevner and Wong-Riley (1993) have also shown that, of the 13 subunits that make up the CO protein, mRNA expression of a mitochondrially encoded subunit (COI) shows greater similarity to CO activity than those subunits that are encoded by nuclear DNA. For example, blobs and layers that show enhanced CO activity are particularly enriched in COI mRNA content but are less enriched in COIV and COVIII mRNA (both are encoded by the nucleus).

It is not surprising that the pattern of cyt b expression shows such parallels to COI mRNA expression, because both are encoded by the mitochondrial genome and, indeed, may be cotranscribed to produce proteins that are key participants in oxidative metabolism (Attardi and Schatz, 1988). The results of Hevner and Wong-Riley (1993) with COI suggest that mitochondrial gene regulation may play a major role in controlling CO activity. Our results with cyt b, although it is not a component of the CO holoenzyme, may be used to extend this notion and generalize a transcriptional linkage between the entire family of mitochondrial genes and CO activity. If this is the case, then such a relationship should assure a similar correspondence in anatomical localization of the various mitochondrial gene products as well as in activity-guided regulation of expression.

Subcellular localization of cyt b mRNA

The dig-ISHH staining procedure, when it was used alone, produced cyt b labeling in cell bodies, as indicated by a stained cytoplasmic ring around a negatively stained nucleus, at all levels within striate cortex. Our observation of weak neuropil staining, which was evident in layers 2/3, 4C, and 6, suggested that cyt b mRNA may be present in dendritic processes as well. This would be consistent with the finding of Hevner and Wong-Riley (1991) that COI is also present in dendrites. According to their model, CO synthesis occurs largely in the cell body and, to a smaller degree, in dendrites, where mitochondrial subunits combine with excess nuclear subunits. The presence of mitochondrial gene products in the neuropil, such as COI and cyt b mRNA, supports this scheme because of their coordinate expression as a single polycistronic unit (Attardi and Schatz, 1988).

Our use of a double-staining procedure showing coexpression of cyt b mRNA and Zif268 protein revealed that neurons were the predominant cell class expressing cyt b. It has been previously shown that Zif268 is primarily expressed in excitatory neurons (Chaudhuri et al., 1995). However, the presence of single-labeled cells (cyt b only) may reflect expression within other classes of cells, e.g., inhibitory neurons, that are not labeled by Zif268 immunostaining. Although it is theoretically possible to confirm this by double-labeling with markers for inhibitory neurons, such as calbindin and parvalbumin (Blumcke et al., 1990; van Brederode et al., 1990), the cytoplasmic locus of these products would obscure staining of cyt b mRNA in any double-labeled cells. Rather, transcription factors that are specific to inhibitory neurons and are confined to the nucleus could provide the spatial contrast necessary for codetection of both products. Unfortunately, such a counterpart to Zif268 has not yet been identified.

Activity-dependent regulation of cyt b

Our finding of cyt b mRNA down-regulation in cortical regions deprived of afferent stimulation fortifies the notion that induction of the mitochondrial gene family as a whole is controlled by functional activity. The cyt b results in visual cortex are consistent with previous findings in muscle tissue where a significant increase in its levels was seen after prolonged stimulation (Williams et al., 1987). However, it is the similarity with COI dependence on activity reported by Hevner and Wong-Riley (1993) that is most intriguing. They found that adult animals treated with monocular deprivation showed striking decrements in COI mRNA staining in geniculate layers and OD columns representing the deprived eye. Furthermore, removal of visual input decreased COI mRNA levels more than CO activity itself—an effect similar to our observation with cyt b—whereas mRNA levels of nuclear CO subunits were less affected.

This has certain implications for transcriptional control of mitochondrial genes and whether nuclear signals may direct this process. It seems unlikely that changes in mitochondrial DNA replication as a whole (Williams, 1986; Williams et al., 1986) are the major regulatory event in brain tissue, because total mitochondrial DNA is reduced by only half as much as COI mRNA after visual deprivation (Hevner and Wong-Riley, 1993). Alternatively, transcriptional events in the mitochondrial genome may be initiated during CO assembly as the need arises for production of the mitochondrial subunits for completion of protein synthesis, thereby affecting the levels of all mitochondrial genes, including cyt b. If this is the case, then one would expect proportional effects in nuclear and mitochondrial CO subunit mRNA levels under conditions of monocular visual exposure. Again, Hevner and Wong-Riley (1993) reported that COI mRNA levels were down-regulated by two to three times the levels of the nuclear subunits and that regional variations in COI staining were more faithful to CO activity than any of the other subunits. Together, these results imply that either the rate of mitochondrial transcription and/or some form of posttranscriptional stabilization is affected by neuronal activity, possibly by second- or third-messenger systems whose induction or activation is guided by synaptic stimulation.

Our finding of differences in CO activity and cyt b mRNA levels after long-term visual deprivation (3 months) further suggests some form of independent control of mitochondrial gene expression or of posttranscriptional events, such as differential mRNA stabilization. Alternatively, the cyt b staining profile may reflect pathological change in V1 due to the unilateral enucleation procedure. In either case, it is intriguing that the intense down-regulation of CO activity is not accompanied by a similar effect on cyt b levels under such conditions. It would be interesting to compare these findings with the levels of COI mRNA, which would also be expected to show effects similar to those of CO because of their close correspondence in the normal brain and after short-term visual deprivation. If so, then differences in posttranscriptional stabilization would emerge as the most likely mechanism because of the polycistronic nature of mitochondrial gene expression. Whatever the reasons for the difference in CO activity and cyt b expression, it is tempting to speculate that prolonged visual deprivation can engage regulatory events in the mitochondrial genome that may participate in the molecular coordination of cortical plasticity.

ACKNOWLEDGMENTS

We thank S. Prasad and M.S. Cynader for help in the preparation of the LGN cDNA libraries. We also thank K. Matsoukas for technical assistance and photography. This work was supported by research grants from the Medical Research Council of Canada (MRC-MA12685) and the Natural Sciences and Engineering Research Council of Canada (NSERC-OGP0155482) to A.C. L.K. was supported by Visiting Research Fellowships from NSERC, FRSQ, and HFSP. A.C. is an MRC Scholar and an Alfred P. Sloan Research Fellow.

LITERATURE CITED

Altschul, S.F., W. Gish, W. Miller, E.W. Myers, and D.J. Lipmean (1990) Basic local alignment search tool. J. Mol. Biol. *215:*403–410.

Attardi, G., and G. Schatz (1988) Biogenesis of mitochondria. Annu. Rev. Cell Biol. *4:*289–333.

Blumcke, I., P.R. Hof, J.H. Morrison, and M.R. Celio (1990) The distribution of parvalbumin in the visual cortex of Old World monkeys and humans. J. Comp. Neurol. *301:*417–432.

Chaudhuri, A., S.S. Prasad, and M.S. Cynader (1993) Patterns of gene expression as determinants of cortical specificity in the monkey visual system. Soc. Neurosci. Abstr. *19:*1799.

Chaudhuri, A., J.A. Matsubara, and M.S. Cynader (1995) Neuronal activity in primate visual cortex assessed by immunostaining for the transcription factor Zif268. Vis. Neurosci. *12:*35–50.

Chomczynski, P., and M. Sacchi (1987) Single step method of RNA isolation by acid guanidinium thiocyanate-phenol-chlorophorm extraction. Anal. Biochem. *162:*156–159.

Clayton, D.A. (1984) Transcription of the mitochondrial genome. Annu. Rev. Biochem. *53:*573–594.

Dyck, R.H., and M.S. Cynader (1993) An interdigitated columnar mosaic of cytochrome oxidase, zinc, and neurotransmitter-related molecules in cat and monkey visual cortex. Proc. Natl. Acad. Sci. USA *90:*9066–9069.

Gadaleta, G., G. Pepe, G. De Candia, C. Quagliariello, E. Sbisa, and C. Saccone (1989) The complete nucleotide sequence of the *Rattus norvegicus* mitochondrial genome: Cryptic signals revealed by comparative analysis between vertebrates. J. Mol. Evol. *28:*497–516.

Hedrick, S.M., D.I. Cohen, E.A. Nielsen, and M.M. Davis (1984) Isolation of cDNA clones encoding T cell-specific membrane-associated proteins. Nature *308:*149–153.

Hevner, R.F., and M.T.T. Wong-Riley (1990) Regulation of cytochrome oxidase protein levels by functional activity in the macaque monkey visual system. J. Neurosci. *10:*1331–1340.

Hevner, R.F., and M.T.T. Wong-Riley (1991) Neuronal expression of nuclear and mitochondrial genes for cytochrome oxidase (CO) subunits analyzed by in situ hybridization: Comparison with CO activity and protein. J. Neurosci. *11:*1942–1958.

Hevner, R.F., and M.T.T. Wong-Riley (1993) Mitochondrial and nuclear gene expression for cytochrome oxidase subunits are disproportionately regulated by functional activity in neurons. J. Neurosci. *13:*1805–1819.

Hevner, R.F., R.S. Duff, and M.T.T. Wong-Riley (1992) Coordination of ATP production and consumption in brain: Parallel regulation of cytochrome oxidase and Na^+, K(+)-ATPase. Neurosci. Lett. *138:*188–192.

Horton, J.C. (1984) Cytochrome oxidase patches: A new cytoarchitectonic feature of monkey cortex. Phil. Trans. R. Soc. [London] *304:*199–253.

Horton, J.C., and D.H. Hubel (1981) Regular patchy distribution of cytochrome-oxidase staining in primary visual cortex of macaque monkey. Nature *292:*762–764.

Kaczmarek, L., B. Kaminska, S. Larocque, and A. Chaudhuri (1995) Molecular characterization of genes derived from monkey LGN cDNA library. Soc. Neurosci. Abstr. *21:*51.

Kadenbach, B., L. Kuhn-Nentwig, and U. Buge (1987) Evolution of a regulatory enzyme: Cytochrome-c oxidase (complex IV). Curr. Topics Bioenerg. *15:*113–161.

Kaminska, B., R.K. Filipkowski, G. Zurkowska, W. Lason, R. Przewlocki, and L. Kaczmarek (1994) Dynamic changes in composition of the AP-1

transcription factor DNA binding activity in rat brain following kainate induced seizures and cell death. Eur. J. Neurosci. *6:*1558–1566.

Morgan, J.I., and T. Curran (1991) Stimulus-transcription coupling in the nervous system: Involvement of the inducible protooncogenes fos and jun. Annu. Rev. Neurosci. *14:*421–451.

Prasad, S.S., and M.S. Cynader (1994) Identification of cDNA clones expressed selectively during the critical period for visual cortex development by subtractive hybridization. Brain Res. *639:*73–84.

Rosa, M.G.P., R. Gattass, and J.G.M. Soares (1991) A quantitative analysis of cytochrome oxidase-rich patches in the primary visual cortex of Cebus monkeys: Topographic distribution and effects of late monocular enucleation. Exp. Brain Res. *84:*195–209.

Struhl, K. (1991) Mechanisms for diversity in gene expression patterns. Neuron *7:*177–181.

Tzagaloff, A., and G. Macino (1979) Mitochondrial genes and translation products. Annu. Rev. Biochem. *48:*419–441.

van Brederode, J.F.M., K.A. Mulligan, and A.E. Hendrickson (1990) Calcium-binding proteins as markers for subpopulations of GABAergic neurons in monkey striate cortex. J. Neurol. *298:*1–22.

Van Itallie, C.M. (1990) Thyroid hormone and dexamethasone increase the levels of a messenger ribonucleic acid for a mitochondrially encoded subunit but not for a nuclear-encoded subunit of cytochrome oxidase. Endocrinology *127:*155–168.

Van Itallie, C.M., S. Van Why, G. Thulin, M. Kashgarian, and N.J. Siegel (1993) Alterations in mitochondrial RNA expression after renal ischemia. Am. J. Physiol. *265:*712–719.

Wiesner, R.J., V. Aschenbrenner, J.C. Ruegg, and R. Zak (1994) Coordination of nuclear and mitochondrial gene expression during the development of cardiac hypertrophy in rats. Am. J. Physiol. *267:*229–235.

Williams, R.S. (1986) Mitochondrial gene expression in mammalian striated muscle. Evidence that variation in gene dosage is the major regulatory event. J. Biol. Chem. *261:*12390–12394.

Williams, R.S., and W. Harlan (1987) Effects of inhibition of mitochondrial protein synthesis in skeletal muscle. Am. J. Physiol. *253:*866–871.

Williams, R.S., S. Salmons, E.A. Newsholme, R.E. Kaufman, and J. Mellor (1986) Regulation of nuclear and mitochondrial gene expression by contractile activity in skeletal muscle. J. Biol. Chem. *261:*376–380.

Williams, R.S., M. Garcia-Moll, J. Mellor, S. Salmons, and W. Harlan (1987) Adaptation of skeletal muscle to increased contractile activity. Expression nuclear genes encoding mitochondrial proteins. J. Biol. Chem. *262:*2764–2767.

Wong-Riley, M.T.T. (1989) Cytochrome oxidase: An endogenous metabolic marker for neuronal activity. Trends Neurosci. *12:*94–101.

Wong-Riley, M.T.T., and E.W. Carroll (1984) Effect of impulse blockage on cytochrome oxidase activity in monkey visual system. Nature *307:*262–264.

Wong-Riley, M.T.T., S.C. Tripathy, T.C. Trusk, and D.A. Hoppe (1989) Effect of retinal impulse blockage on cytochrome oxidase-rich zones in the macaque striate cortex: I. Quantitative electron-microscopic (EM) analysis of neurons. Vis. Neurosci. *2:*483–497.